Received: 20 December 2021 | Accepted: 20 June 2022

DOI: 10.1002/pros.24451

ORIGINAL ARTICLE

The Prostate WILEY

Proteoglycans orchestrate remodeling of prostatic cytoarchitecture after androgenic blockade in old gerbils

Silvana G. P. Campos PhD[1] | Bianca F. Gonçalves PhD[1] | Thalles Fernando Rocha Ruiz MSc[2] | Ellen Cristina R. Leonel PhD[3] | Daniele L. Ribeiro PhD[4] | Luiz Roberto Falleiros Junior MSc[5] | Rejane M. Goes PhD[1] | Sebastião R. Taboga PhD[1]

[1]Department of Biological Sciences, Institute of Biosciences, Humanities and Exact Sciences, São Paulo State University (Unesp), São José do Rio Preto, São Paulo, Brazil

[2]Department of Structural and Functional Biology, State University of Campinas (UNICAMP), Campinas, São Paulo, Brazil

[3]Department of Histology, Embryology and Cell Biology, Institute of Biological Sciences, Federal University of Goiás (UFG), Goiânia, Goiás, Brazil

[4]Department of Cell Biology, Histology and Embriology, Institute of Biomedical Sciences-ICBIM, Federal University of Uberlândia (UFU), Uberlândia, Minas Gerais, Brazil

[5]Department of Urology, São José Rio Preto School of Medicine (FAMERP), São José do Rio Preto, São Paulo, Brazil

Correspondence

Silvana G. P. Campos, PhD, Department of Biological Sciences, Institute of Biosciences, Humanities and Exact Sciences, São Paulo State University (Unesp), Rua Cristóvão Colombo, 2255, Jardim Nazareth, São José do Rio Preto, São Paulo 15054-000, Brazil.
Email: spegorin@hotmail.com

Funding information

Conselho Nacional de Desenvolvimento Científico e Tecnológico; Fundação de Amparo à Pesquisa do Estado de São Paulo

Abstract

Background: The aim of this study was to evaluate modifications in proteoglycan morphology and composition in the prostatic stroma of 18-month-old gerbils after surgical castration, in association or not with an androgenic blockade.

Methods: The animals ($n = 5$) were sorted into groups subjected or not to antiandrogen treatment (flutamide 10 mg/kg/day) administered for the total postsurgery period and euthanized at 7- or 30-day postcastration; the control group consisted of intact animals. Tissue analysis included immunohistochemical assessment (perlecan and chondroitin sulfate) and proteoglycan morphology was analyzed by transmission electron microscopy.

Results: Chondroitin sulfate frequency was increased 7 days postcastration with an androgenic blockade. The presence of these carbohydrates was rare after 30 days of androgenic blockade treatment. There was a significant increase in the amount of perlecan in the prostate stroma from groups subjected to castration plus flutamide for 7 or 30 days. Ultrastructural analysis showed that the incidence of areas occupied by proteoglycans and basement membrane was altered by treatment. In addition, androgenic blockade results in changes in the amount, thickness, and morphology of these structures. At 30 days postcastration, with or without flutamide treatment, larger proteoglycans were common.

Conclusions: In this study, in particular, the decrease in chondroitin sulfate after the longer period might be understood as a prostatic response to androgenic deprivation, while the high frequency and permanence of perlecan led to the assumption that its modulation could be androgen-independent. Length and form alterations in proteoglycans as well as associations among them and with the basement membrane were dynamic events in the prostate microenvironment.

KEYWORDS

castration, chondroitin sulfate, flutamide, perlecan, prostate

1 | INTRODUCTION

Surgical or chemical castration is the standard systemic therapy for patients with advanced prostate cancer.[1] Most prostate cancers initially respond to androgen ablation therapy due to hormone dependence for growth, but the emergence of hormone-independent cancer cells can occur, meaning that androgen ablation is ineffective at this stage.[2,3] Thus, the androgen deprivation strategy used as early intervention may delay the promotion and/or progression of prostate cancer. One potential suppressive agent is nonsteroidal antiandrogen flutamide, which exerts effects by interfering with the binding of dihydrotestosterone or testosterone to the androgen receptor.[4] Currently, there are indications that flutamide as a second-line hormonal therapy decreases adrenal androgens and is effective for bicalutamide-refractory prostate cancer.[5]

Prostate homeostasis requires bidirectional signaling between epithelial cells and stromal compounds, including fibroblasts and smooth muscle cells, vasculature, soluble mediators, and extracellular matrix (ECM) proteins.[6] In this aspect, androgen ablation therapy promotes prostatic structural regression, mainly attributed to a decrease in secretory activity and a reduction in the number of luminal epithelial cells by apoptosis.[7,8] Structural alterations also occur at the stroma level following castration, called stromal remodeling, accompanied by a functional alteration in the prostatic fibromuscular stromal environment.[9] This is due to an inherent plasticity to respond rapidly to emerging situations, such as in wound repair and disrupted homeostasis.[10]

Regarding the ECM, it is composed of a basement membrane and interstitial matrix, both of which contain fibrous proteins and numerous proteoglycans.[11] The latter contribute to various biological functions such as the maintenance of tissue structure and regulation of cell proliferation, adhesion, migration, and differentiation.[12] The proteoglycans expression is regulated in a temporal and spatial manner in physiological and pathological processes.[13] Additionally, the prostate is an abundant secretor of glycoproteins of all types, and alterations in glycans[14] are, therefore, attractive as modulators of stromal plasticity and, as potential biomarkers. Under hormonal blockade conditions, increased deposition of ECM structural proteins was observed.[15,16]

Among these molecules, proteoglycans are abundant at the cell surface and ECM in any tissue, and both core protein and polysaccharide chains contribute to the functional activity of these glycoproteins.[17] Glycosaminoglycans polysaccharide chains are an essential part of the matured proteoglycans molecules and principal contributor to the proteoglycans functional properties.[18] Chondroitin sulfate is a glycosaminoglycan side chain component of several distinct proteoglycans and in humans, it is increased in the peritumoral stroma of prostate tumors in an advanced stage.[19,20] Perlecan/heparan sulfate proteoglycan is an extracellular proteoglycan that binds and cross-links multiple ECM components providing tissue organization and matrix stabilization,[21] and its behavior under androgenic blockade conditions is of particular interest for the study of prostate pathological mechanisms.

Our research group adopted the gerbil, *Meriones unguiculatus*, as an alternative experimental model for a prostate cancer study. This rodent model has been providing a good alternative to study the alterations that occur in the prostate since it develops spontaneous and induced neoplasia.[8,22–24] How the response to androgens, or to androgen withdrawal, may be significantly influenced by age, we have previously evaluated the effects of castration in old gerbils (*M. unguiculatus*).[25,26] Like other mammals, the stromal compartment of the gerbil prostate responds to steroidal ablation with a pattern of phenotypic alterations. An accumulation of ECM elements under the epithelium is evident, smooth muscle cells and fibroblasts exhibit secretory phenotypes.[25,27,28] In studies with androgen blockade we used, in addition to surgical castration, the chemical blockade with flutamide. The gerbil has a high production of androgens by the adrenal glands, which could compensate for the drop in testicular androgen production. Endogenous testosterone levels in 18-month-old animals are around 2800 pg/ml[29] compared to 1865 pg/ml in 6-month-old Lobund-Wistar rats and 1236 pg/ml in Copenhagen rats.[30] In addition, the correlation between hormonal changes and proteoglycan expression and deposition remains unclear. Thus, the aim of the present study was to evaluate the prostatic stroma of old gerbils (18 months) after the androgenic blockade, focusing on the remodeling pattern of proteoglycans derived from chondroitin sulfate and heparan sulfate.

2 | MATERIAL AND METHODS

2.1 | Animals and experimental design

The animals (18 months old) were divided into 5 groups ($n = 5$ per group) and were handled in accordance with the Institutional guidelines. The experiment was approved by the Animal Experimentation Ethics Committee of São Paulo State University (protocol number: 004/06 – ECEA). The gerbils were housed in plastic cages (three to five animals per cage), under controlled environmental conditions (25°C, 40%–70% relative humidity, 12 light/12 dark), and supplied with water and balanced chow ad libitum. Two groups were subjected to castration and euthanized 7 or 30 days after surgery. Two other groups were castrated and subsequently received antiandrogen treatment (flutamide, 10 mg/kg/day, Sigma Chemical) for 7 (castrated plus flutamide 7 days) or 30 (castrated plus flutamide 30 days) days after surgery, and then euthanized. The control group was composed of intact animals. Vegetable oil in the volume of 0.1 ml/application/animal was applied as the flutamide dilution vehicle.

2.2 | Histopathological analysis

Euthanasia was performed by insensibilization by carbon dioxide followed by decapitation. The ventral lobe of each gerbil prostate was collected and fixed for 24 h in 4% paraformaldehyde diluted in

phosphate-buffered saline; then the tissue was washed, dehydrated, cleared in xylene, and embedded in paraffin (Histosec™; Merck). Serial sections (5 µm thickness) were subjected to cytochemical staining with hematoxylin-eosin for general tissue evaluation before histopathological classification and immunohistochemical analyses. Tissue sections were analyzed using an Olympus photomicroscope (Olympus) and images were acquired using the Image-Pro-Plus software version 4.5 for Windows™ (Media Cybernetics Inc.).

2.3 | Immunohistochemistry analysis

Before immunohistochemical assays, the antigen retrieval was performed by incubating the sections at 92°C in citrate buffer of pH 5.0 for 20 min. Briefly, slides were treated with 3% H_2O_2 in methanol for 20 min to quench the endogenous peroxidase activity and then incubated in horse serum 1% in PBS for 1 h to block nonspecific binding. Primary antibodies applied were mouse anti-human chondroitin sulfate (CS-56; Sigma Chemical Co.; 1:500) for 1 h at room temperature and rat monoclonal perlecan (A7L6, Santa Cruz Biotech.; 1:50), overnight at 4°C. Next, the sections were incubated for 45 min with a biotinylated horse anti-mouse secondary antibody, followed by peroxidase-labeled avidin/biotin solution reaction (1:250, NovoStain Super ABC Kit; Novocastra) for 45 min. Finally, they were exposed to the peroxidase substrate DAB for 3 min, stained in methyl green or hematoxylin, and mounted.

2.4 | Evaluation of immunoreaction of the ECM components

To determine the relative frequency of prostatic stromal components (chondroitin sulfate, perlecan, and blood vessels—microvessel frequency determination), histological sections were subjected to analysis using the Weibel system of multipoint counting.[31] Briefly, 20 microscopic fields were obtained and randomly selected in each group (five animals per group). The relative frequency (%) was calculated by counting the points that corresponded precisely to the DAB-stained area.

2.5 | Ultrastructural cytochemistry for proteoglycans

Ventral prostate samples for ultrastructural analysis were treated with cuprolinic blue, which stains all the proteoglycans in tissues. A critical eletrolitic concentration which preserves proteoglycans.[32,33] Briefly, prostatic fragments were fixed in 2.5% glutaraldehyde (Electron Microscopy Sciences) in 0.025 M sodium acetate buffer pH 5.6 (Sigma Chemical), with 0.3 M magnesium chloride (Sigma Chemical), for 30 min at 4°C. After this prefixation, fragments were fixed overnight at room temperature, in the same prefixation solution with 0.2% Cuprolinic Blue (Electron Microscopy Sciences). After washing in acetate buffer with the same concentration of magnesium chloride (Sigma Chemical), fragments were immersed in 1% phosphotungstic acid (Sigma Chemical) for 30 min and then dehydrated and embedded in Araldite (Polysciences Inc.). Then ultrathin sections (70 nm) were prepared by an EM UCT ultramicrotome (Leica Microsystems), contrasted with 2% alcoholic uranil acetate (SPI-Chem Inc.) followed by 2% lead citrate (Merck KGaA) in sodium hydroxide solution and observed and evaluated with an LEO–Zeiss 906 Transmission Electron Microscope at 60 kV. With this method, proteoglycans appear as electron-dense structures, granulous or filamentous, depending on the size of the proteic core as well as on the size, quality, and number of glycosaminoglycans chains.[34]

2.6 | Morphometrical analysis

The thickness of the basement membrane and length of proteoglycans associated with the basement membrane were measured using electronmicrographs at 21,560×, magnification, captured with a resolution of 660 dpi. We used 6–11 fragments per group ($n = 3$ animals/group). The thickness of the acinar basement membrane and the length of proteoglycans were analyzed at 30 different points per group and then the mean value was calculated (nm). The morphometric analysis was carried out using Image-Pro Plus version 4.5 for Windows software.

Quantitative analyses of fibrillar components of the ECM and associated with the basement membrane were performed to determine the presence of high/eletrondense (larger) or less aggregated proteoglycans (small), and collagen type I, in the cuprolinic blue technique. Relative frequency (%) was quantified using an adapted M130 multipoint test system.[31] Five electromicrographs (21,560× magnification) from each group were randomly selected to measure the distribution of these elements. The frequency was expressed as a percentage of total points.

2.7 | Statistical analysis

The statistical analyses were performed with StatisticaStatistica 6.0 software (Statsoft Inc.). For comparisons of results among experimental groups, data were checked using the Kolmogorov-Smirnov normality test. One-way analysis of variance with posteriori Tukey's test was performed, according to the characteristics of each variable. $p \leq 0.05$ was considered statistically significant.

3 | RESULTS

3.1 | Morphological and stereological analyses

Tissue locations of chondroitin sulfate and perlecan were determined by immunohistochemistry in the prostate gland (Figures 1 and 2). Chondroitin sulfate, perlecan, and blood vessel frequencies were

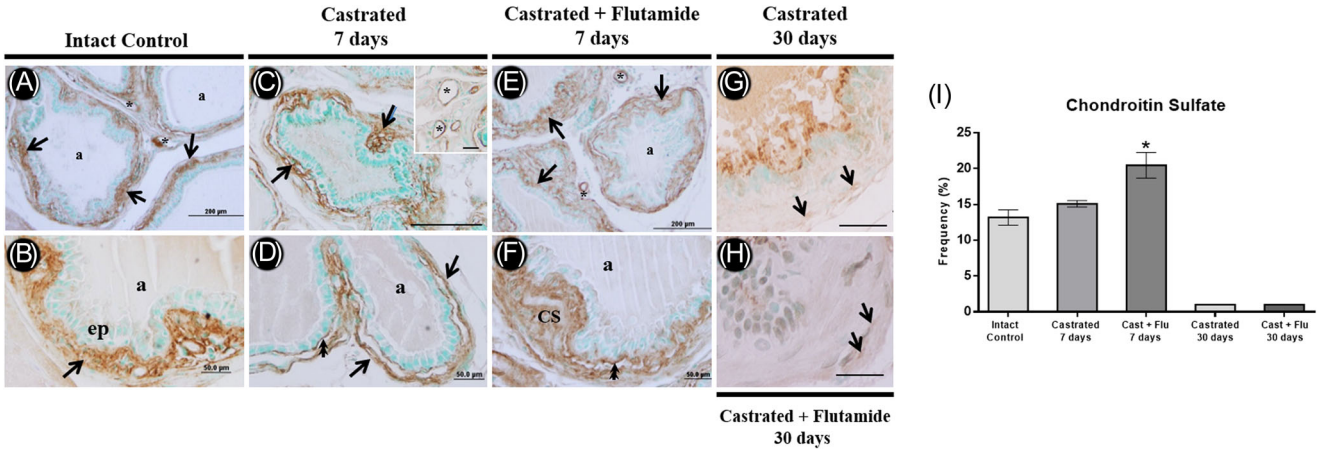

FIGURE 1 Chondroitin Sulfate (CS) were modulated in the prostate stroma after castration and androgenic blockade. Immunoreactive areas (brown) indicate the distribution of the proteoglycan (arrows) around the prostatic acini (a). (A) and (B) Intact group presented uniform distribution of CS in subepithelial region and muscular stroma. Compared to 7 days postcastration (C) and (D), androgenic blockade at the same period (E) and (F) showed increased deposition of CS in a wavelike distribution and associated to basement membrane (double arrow). *C inset*: presence of CS in the blood vessel wall (asterisks) in the prostatic stroma. At 30 days postcastration, without (G) or with androgenic blockade (H), CS were scarce in prostate stroma. (I) Frequency of CS among treatments. Values represent mean ± SEM (n = 5 per group). The asterisk indicates significant difference between the groups analyzed ($p \leq 0.05$). Statistical analysis based on the ANOVA and Tukey's test. Experimental Groups: (A) and (B) Intact control. (C) and (D) Castrated—7 days. (E) and (F) Castrated plus flutamide—7 days. (G) Castrated—30 days. (H) Castrated plus flutamide – 30 days. a, acinus; ANOVA, analysis of variance; asterisks, blood vessels; ep, epithelium. Immunostaining of chondroitin sulfate counterstained with methyl green. [Color figure can be viewed at wileyonlinelibrary.com]

obtained by immunohistochemical evaluation (Figures 1I and 2F,G). There was a significant increase in the frequency of blood vessels in castrated animals 30 days after surgery, while the other groups showed values similar to intact controls (Figure 2G).

Chondroitin sulfate was a constant component of the prostatic ECM (Figure 1A–F). Androgenic blockade with flutamide at 7 days postcastration presented an increase in chondroitin sulfate frequency in comparison to intact and castrated (7 days) groups (Figure 1A–F,I). It was present in the subepithelial region, between smooth muscle cells and in the wall of blood vessels, following the wave-like distribution of collagen fibers and smooth muscle cells, as an abundant component of stroma after the androgenic blockade. After 30 days of treatment, the presence of chondroitin sulfate was rare (Figure 1G–I).

The distribution of perlecan was similar to chondroitin in the prostatic stroma of intact controls (Figure 2A). Perlecan was also present as a component of the basement membrane of the acinar structure (Figure 2A). This distribution was observed in the intact control group and maintained in the castrated groups after 7 and 30 days (Figure 2B,C). Castrated animals only showed a higher incidence of perlecan 30 days after surgery, when compared to the control group (Figure 2F). However, there was a significant increase in the amount of perlecan in the prostate stroma from groups subjected to castration plus flutamide for 7 or 30 days compared to the control group and circumventing the smooth muscle cells and blood vessels (Figure 2D–F). However, 30 days after the castration plus flutamide, the distribution of perlecan was no longer concentric and continuous around the acini and presented a thinner and more dispersed pattern (Figure 3E).

3.2 | Transmission electron microscopy analyses of prostatic proteoglycans

In the epithelium-stroma interface, fine electron-dense filaments were observed in association with the basement membrane. Among them, short proteoglycans were periodically disposed in the basement membrane, and larger ones showed a widespread distribution. The structural organization of fibrous connective tissue and basement membrane in the periacinar region of the prostate was evaluated. Prostatic tissue from animals of the intact control group showed epithelium lying on a thick basement membrane, associated with proteoglycans (identified as electron-dense filaments) on its surface, with anchoring points for type I collagen on the dense lamina region (Figure 3A,B). Proteoglycan organization showed a perpendicular positioning to the collagen fiber bundles in the stroma (Figure 3B). Other regions of the ECM adjacent to the epithelium were composed of depositions of amorphous material and cellular projections of stromal cells (Figure 3A,B).

The incidence of areas occupied by proteoglycans and by a basement membrane (Table 1) was altered by the treatment performed, resulting in changes in the amount, thickness, and morphology of these structures (Figure 3C–J). The thickness of the basement membrane significantly decreased after 7 days of treatment and recovered after 30 days in the castrated group, whereas in the castrated plus flutamide group this aspect was not reversed (Table 1).

Small proteoglycan lengths associated with the basement membrane did not vary in the prostate from treated groups when

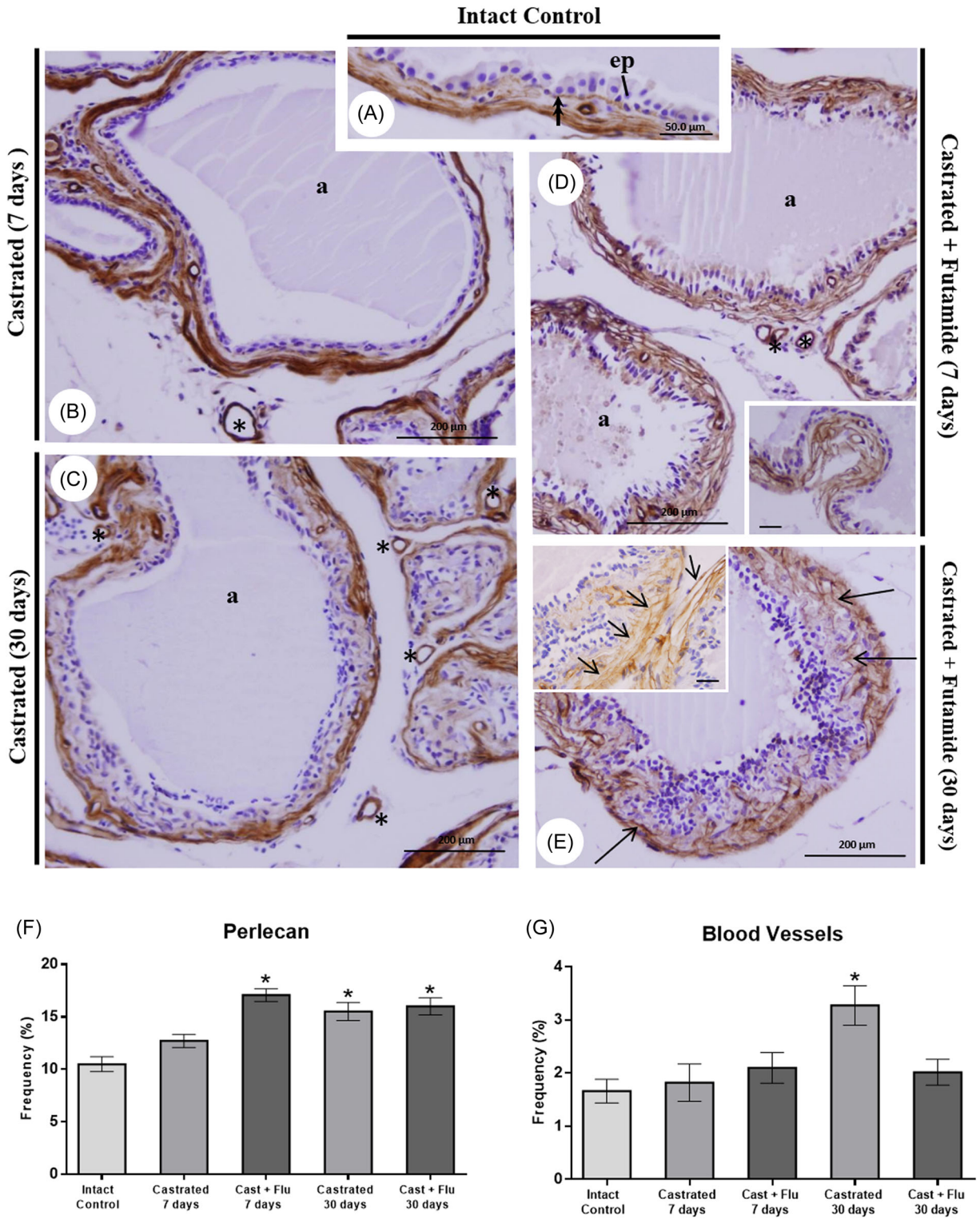

FIGURE 2 Perlecan deposition in the prostate stroma after castration and androgenic blockade. Immunoreactive areas (brown) indicate the distribution of perlecan around the prostatic acini (a). (A) Intact groups showed a perlecan- enriched stroma, also associated to basement membrane (double arrows). At 7 days (B) and 30 days (C) after surgery, perlecan distribution were maintained with evident blood vessels (asterisks), mainly in 30 days. Flutamide treatment promoted no significant distribution of perlecan at 7 days (D), but an increase and sparse deposition of these proteoglycans at 30 days (E) were observed. Note in the insets of (D) and (E) fragmented and thinner perlecan deposits. (F) Frequency of perlecan and (G) blood vessels among treatments. Values represent mean ± SEM (n = 5 per group). The asterisk indicates significant difference between the groups analyzed ($p \leq 0.05$). Statistical analysis based on the ANOVA and Tukey's test. Experimental Groups: (A) Intact control; (B) Castrated—7 days; (C) Castrated—30 days; (D) Castrated plus flutamide—7 days; (E) Castrated plus flutamide—30 days. Immunostaining of perlecan counterstained with hematoxylin. ANOVA, analysis of variance. [Color figure can be viewed at wileyonlinelibrary.com]

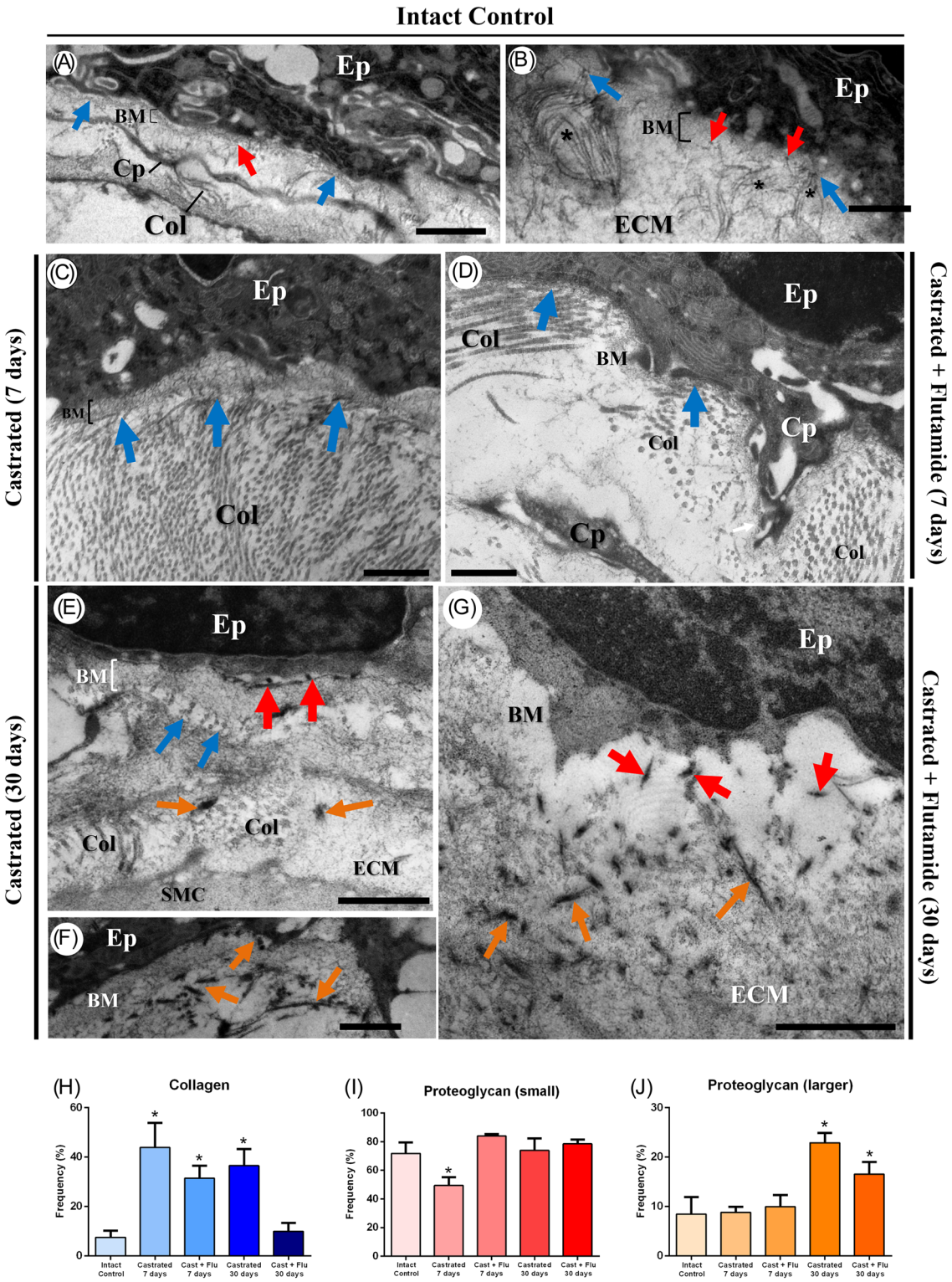

FIGURE 3 Ultrastructural changes in the prostatic stroma after castration and/or flutamide treatment. (A) and (B) Periglandular region in which the basement membrane (BM) was associated with different proteoglycans, which can be identified by the length, thickness, and type of association with BM (red arrows). Collagen fibrils anchoring points associated to proteoglycans in the BM (blue arrows) were observed. (C) and (D) Electron-dense basement membrane (BM) were associated proteoglycans (thin arrows) and collagen fibrils (Col) in 7 days postcastration. Anchoring regions were also observed (blue arrows). Thinner and discontinuous BM were observed after 7 days postcastration plus androgen blockade treatment (in D). Citoplasmatic projection (Cp) were observed in this group. (F–H) More electron-dense proteoglycans were observed associated with BM (red arrows) and in the stroma and extracellular matrix (ECM) (orange arrows) in both groups at 30 days. Multiple collagen (Col) anchorage points (blue arrows) were observed in 30 days postcastration group. Dense and filamentous proteoglycans (orange arrows) were enhanced in 30 days postcastration plus flutamide treatment. (H–J) Frequency (%) of collagen and proteoglycans (small and larger). Values represent mean ± SEM ($n = 5$ per group). The asterisk indicates significant difference between the groups analyzed ($p \leq 0.05$). Statistical analysis based on the ANOVA and Tukey's test. Scale Bars: 0.56 µm. ANOVA, analysis of variance; Ep, epithelium; SMC, smooth muscle cell. [Color figure can be viewed at wileyonlinelibrary.com]

compared to the controls (Table 1). Similarly, the frequency of small proteoglycans associated with the basement membrane was also unchanged, with the exception of the 7-day castrated group (Figure 3I). However, the frequency of anchorage sites of collagen I changed (Figure 3H). The collagen layer underlying the basement membrane increased extensively in the groups after 7 days of treatment, became more electron-dense and multiple collagen anchorage points were observed (Figure 3C,D). These aspects remained after 30 days in the castrated group, while the castrated group plus flutamide decreased the amount of collagen fibers associated with the basement membrane (Figure 3H).

At 30 days postcastration, with or without flutamide treatment, larger (from 58 to 116 nm) proteoglycans were common and associated with the basement membrane and scattered among ECM (Figure 3E–G,J). These proteoglycans were more electron-dense than those observed in the 7 days postcastration groups. However, these proteoglycans were rarely observed as long filaments in the 30 days postcastration plus flutamide group, in comparison to 30 days castrated group. In addition, at 30 days postcastration plus flutamide, the amount of collagen I underlying the epithelium was less evident but the constituents of the fibrillar network of the ECM occupied most of the region and it was denser (Figure 3G).

TABLE 1 Basement membrane morphometric analysis of gerbil prostate in different groups

Time (days) treatments	Basement membrane components	
	Thickness (nm)	Dimension of proteoglycans associated (nm)
Intact control	177.80 ± 8.40	85.07 ± 5.00
7 days castrated	119.30 ± 8.60*	68.15 ± 2.50
7 days Flutamide	127.60 ± 12.30*	55.10 ± 1.70
30 days castrated	180.70 ± 15.74	64.28 ± 3.50
30 days flutamide	113.10 ± 9.00*	83.61 ± 17.50

Note: Values represent mean ± SEM. The asterisks indicate significant differences between the groups analyzed ($p \leq 0.05$). Statistical analysis based on the ANOVA and Tukey-honest significant difference.

4 | DISCUSSION

In the present study, we analyzed the influence of androgenic blockade on the components of the ECM of old Mongolian gerbils as well as the vascular supply in the short and long term. In the old gerbil prostate, the modulation of proteoglycans occurred under androgenic ablation. We evaluated the presence of perlecan and chondroitin sulfate by in situ immunostaining and performed the global analysis of proteoglycans by transmission electron microscopy in the periglandular region and their participation in angiogenesis.

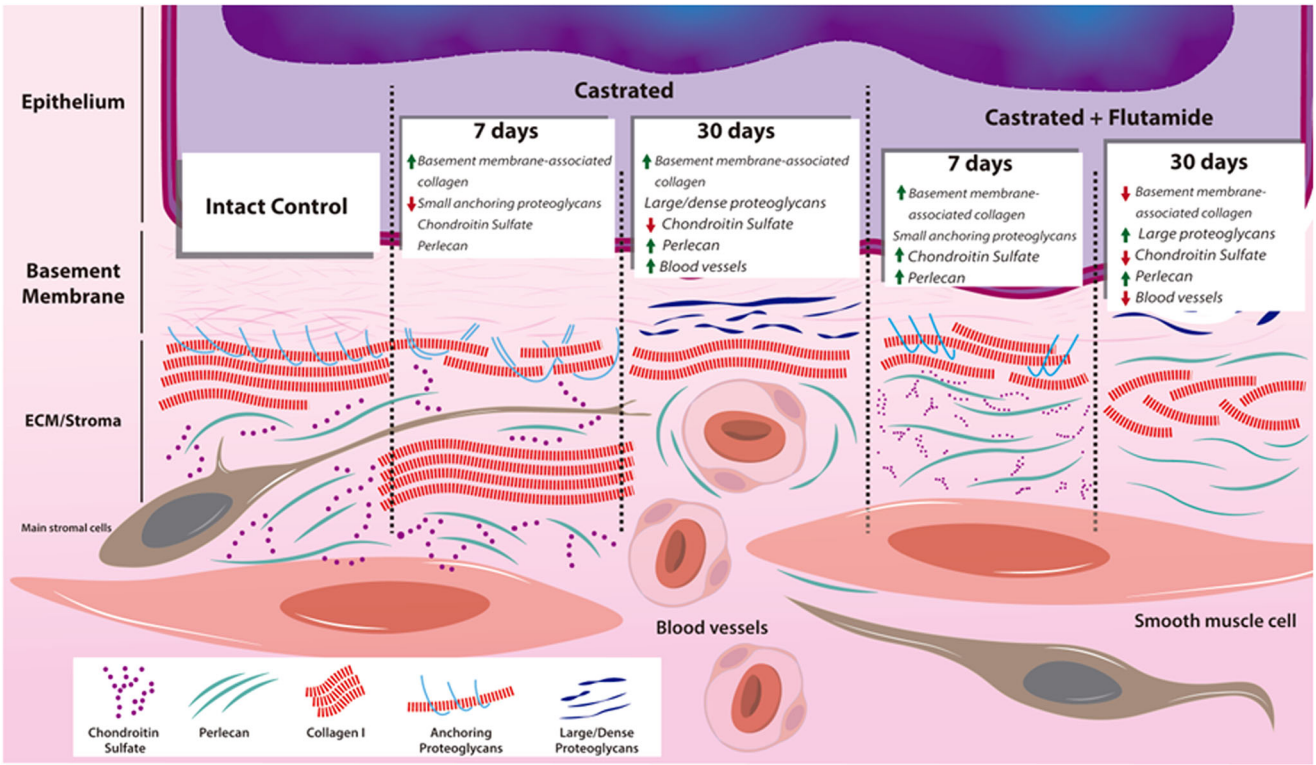

FIGURE 4 Schematic representation. Remodeling of the epithelium-stroma interface after androgenic blockade involves proteoglycans rich in chondroitin and heparan sulfate. Androgenic blockade results in changes in the amount, thickness, morphology of these structures, and in its interaction with the basement membrane, contributing to the maintenance of the prostatic periglandular cytoarchitecture. [Color figure can be viewed at wileyonlinelibrary.com]

Overall, we observed that while androgenic blockade induces an initial regression of prostate cancer, the regressed gland eventually escapes from the therapy, resumes its growth, and maintains a small secretory activity.[9] This aspect is associated with a structural reorganization that adapts to low androgenic levels and has active participation of stromal elements.

The presence of chondroitin sulfate glycosaminoglycan in side chains of proteoglycans in the prostatic stroma was temporally and dynamically modulated in treated animals. During the initial prostatic response, large deposits formed below the glandular epithelium up to 7 days postcastration. In guinea pigs, the highest rates of immunoreactive chondroitin were found in castrated animals, where staining of the periglandular basement membranes was uniformly intense.[35] In rat ventral prostate, a transient increase in high-molecular-mass hyaluronan was observed at 7 days after castration,[36] whereas an apparent increase in heparan sulfate content was observed at 21 days after the androgenic blockade.[37]

In diabetic rats, an increase in chondroitin sulfate in the prostate was also influenced by the reduction in androgens caused by this condition.[38] In human prostate benign proliferative hyperplasia and advanced prostate cancer, the chondroitin sulfate expression is selectively increased in the periacinar region.[20,39,40] The role of proteoglycans rich in chondroitin sulfate is associated with the enhanced assembly of a pericellular matrix and promotes prostate cancer cell motility and invasion in vitro.[41] After 30 days, the amount of chondroitin sulfate decreased in both groups. Structural alterations in glycan chains seem to affect the biological properties of proteoglycans.[42] Furthermore, the identification of glycosylation as a global target for androgen control in the prostate has already been described.[14,43] In the present study, the decrease in chondroitin sulfate after the longer period, in particular, might be understood as a prostatic response to androgenic deprivation and how this condition can be crucial for the properties of ECM.

Studies associating the participation of perlecan in prostatic regeneration after castration are rare. Perlecan plays a structural role in the compact basement membrane underlying the epithelium, where along with collagen IV and laminin, it supports epithelial polarity.[44,45] Perlecan also acts as a signaling molecule, orchestrating the binding and signaling of mitogens and morphogens to cells in a temporal and dynamic fashion.[46] Our data corroborate the importance of perlecan associated with blood flow recovery in the prostate after the androgenic blockade. The positive correlation between perlecan and newly formed microvessels was also observed in prostatic tumor stroma.[47,48] We initially analyzed the blood vessels of the prostatic stroma to describe the damage of androgen deprivation in endothelial cells, which causes ischemia that leads to glandular atrophy, a primary effect of the treatment.[49] As well as epithelial cell apoptosis, the ischemia occurs between 24 and 72 h after the surgical treatment, while after periods of 7 and 30 days, the gland is in recovery or adaptation.[25] Esser et al.[50] observed that in 6–9-month-old mice the expression and localization of perlecan were unchanged in castration/regeneration studies, when a qualitative analysis was performed. Studies on several prostate cancer models correlate high perlecan expression with rapid cell proliferation.[48,51] Furthermore, it was evident that the presence of perlecan acted as a border beneath the epithelium and helped to support epithelial polarity and maintain its differentiated state after the androgenic blockade.

The overall analysis of proteoglycans revealed that the prostrate in old gerbils is rich in proteoglycans associated with the basement membrane, with collagen I fibers, which probably assist the organization of collagen bundles, which increased after 7 days of castration. During this period, the collagen I deposition in the periacinar region showed similarity to the wound repair process. This fibrosis seemed to help maintain the cytoarchitecture of the glandular epithelium. In castration plus flutamide groups, the subepithelial regions with less collagen I fibers allowed the epithelial cells to show cytoplasmic projections toward the stroma, due to basement membrane displacement. In the tumor-associated reactive stroma, the myofibroblasts and carcinoma-associated fibroblasts also remodel the ECM by deposition of collagen type I and other ECM components,[15] showing that this stromal response occurs under different injury conditions in the prostate. It has been reported that versican, a proteoglycan rich in chondroitin, is a candidate for major proteoglycan in prostatic ECM after steroid-induced changes.[35] In our analyses, we also suggested that versican had a marked presence in the ECM after a short period of the androgenic blockade. Future analyses will allow us to prove this possibility.

References to any morphological alterations in the basement membrane in conditions of prostatic injury are scarce and contradictory. In the ventral lobe of adult gerbils, the basement membrane thickness increased after 7 days of castration with or without flutamide treatment.[52] In rats, diabetes led to 25% thickening in the prostate acinar basement membrane, accompanied by an increase in and disorganization of its proteoglycans.[38] In humans, with the increasing Gleason grade, the density and thickness of the basement membrane glycoprotein decreased, with higher fragmentation, which suggests that the basement membrane would be modified by the tumor cells, allowing them to spread locally. In this way, it is believed that the ECM is a gel-like structure that varies in density according to the polymerization degree of the glycoprotein molecules: the greater the polymerization, the denser or more rigid the ECM.[53] In the present study, in the groups evaluated after 7 days of castration, the decrease in basement membrane thickness was directly related to the smaller size of proteoglycans. It is likely that part of the changes in basement membrane thickness is due to the modulation that occurred in perlecan.

Long-term castration promoted the emergence and/or reorganization of proteoglycans in the periacinar region, which were thicker and more electron-dense. Similar data were obtained in the prostate of diabetic rats and the authors stated

that the alterations affected the interactions of proteoglycans with other molecules.[38]

5 | CONCLUSIONS

The results indicated that surgical castration associated with flutamide promotes changes in the prostate architecture of old gerbils and the evaluated proteoglycans participated in the process of glandular rearrangement. Chondroitin sulfate proteoglycans were a prominent component in the subepithelial region in the short term. Perlecan participated not only in the basement membrane structure but also in stromal remodeling and angiogenesis. Substantial changes in proteoglycans occur both in prostate cancer cells and the tumor microenvironment, and this set of events profoundly influences cell proliferation and differentiation in the prostate, reinforcing the importance of this study (Figure 4).[15,54] Additionally, our data point to the gerbil as a good model to evaluate the in vivo prostatic proteoglycan rearrangements during aging and under androgenic blockade conditions, regarding their biological functions, role in specific signaling pathways associated with castration-resistance, and therapeutic potential.

AUTHOR CONTRIBUTIONS

Silvana G. P. Campos, Thalles Fernando Rocha Ruiz, and Sebastião R. Taboga designed the study. Silvana G. P. Campos, Thalles Fernando Rocha Ruiz, and Ellen Cristina R. Leonel wrote the manuscript. Daniele L. Ribeiro and Rejane M. Goes critically appraised the manuscript. Silvana G. P. Campos, Bianca F. Gonçalves, and Luiz Roberto Falleiros Junior performed experiments. Silvana G. P. Campos, Bianca F. Gonçalves, and Thalles Fernando Rocha Ruiz performed data analysis. All authors reviewed the manuscript. Silvana G. P. Campos and Sebastião R. Taboga had access to all of the data in the study and takes responsibility for the integrity of the data and the accuracy of its analysis.

ACKNOWLEDGMENTS

Fundação de Amparo à Pesquisa do Estado de São Paulo—FAPESP (fellowship to S. G. P. C., 06/000215-3; and research financing, 05/04670-4) and Conselho Nacional de Desenvolvimento Científico e Tecnológico—CNPq (research financing, 302938/2020-6, fellowship to S. R. T.).

CONFLICT OF INTEREST

The authors declare no conflict of interest.

DATA AVAILABILITY STATEMENT

The data that support the findings of this study are available from the corresponding author upon reasonable request.

ORCID

Silvana G. P. Campos https://orcid.org/0000-0002-6813-7148
Rejane M. Goes https://orcid.org/0000-0002-3622-460X
Sebastião R. Taboga https://orcid.org/0000-0002-0970-4288

REFERENCES

1. Huggins C, Hodges CV. Studies on prostatic cancer: I. The effect of castration, of estrogen and of androgen injection on serum phosphatases in metastatic carcinoma of the prostate. *J Urol*. 2002;168:9-12.
2. Cunha GR, Donjacour AA, Cooke PS, et al. The endocrinology and developmental biology of the prostate. *Endocr Rev*. 1987;8:338-362. doi:10.1210/edrv-8-3-338
3. Harris WP, Mostaghel EA, Nelson PS, Montgomery B. Androgen deprivation therapy: progress in understanding mechanisms of resistance and optimizing androgen depletion. *Nat Clin Pract Urol*. 2009;6(2):76-85. doi:10.1038/ncpuro1296
4. Denis LJ, Griffiths K. Endocrine treatment in prostate cancer. *Semin Surg Oncol*. 2000;18:52-74. doi:10.1002/(sici)1098-2388(200001/02)18:1<52::aid-ssu8>3.0.co;2-6
5. Nakai Y, Tanaka N, Miyake M, Inoue T, Anai S, Fujimoto K. Response to flutamide, as second-line therapy after bicalutamide, predicts efficacy of abiraterone, not that of enzalutamide. *BMC Res Notes*. 2018;11(1):342. doi:10.1186/s13104-018-3453-z
6. Leach DA, Need EF, Toivanen R, et al. Stromal androgen receptor regulates the composition of the microenvironment to influence prostate cancer outcome. *Oncotarget*. 2015;6(18):16135-16150. doi:10.18632/oncotarget.3873
7. English HF, Santen RJ, Isaacs JT. Response of glandular versus basal rat ventral prostatic epithelial cells to androgen withdrawal and replacement. *Prostate*. 1987;11(3):229-242. doi:10.1002/pros.2990110304
8. Campos SG, Zanetoni C, Scarano WR, Vilamaior PS, Taboga SR. Age-related histopathological lesions in the Mongolian gerbil ventral prostate as a good model for studies of spontaneous hormone-related disorders. *Int J Exp Pathol*. 2008;89:13-24. doi:10.1111/j.1365-2613.2007.00550.x
9. Shidaifat F, Daradka M, Al-Omari R. Effect of androgen ablation on prostatic cell differentiation in dogs. *Endocr Res*. 2004;30(3):327-334. doi:10.1081/erc-200033196
10. Barron DA, Rowley DR. Microenvironment and prostate cancer progression. *Endocr Relat Cancer*. 2012;19(6):R187-R204. doi:10.1530/ERC-12-0085
11. Frantz C, Stewart KM, Weaver VM. The extracellular matrix at a glance. *J Cell Sci*. 2010;123(Pt 24):4195-4200. doi:10.1242/jcs.023820
12. Theocharis AD, Skandalis SS, Tzanakakis GN, Karamanos NK. Proteoglycans in health and disease: novel roles for proteoglycans in malignancy and their pharmacological targeting. *FEBS J*. 2020;277(19):3904-3923. doi:10.1111/j.1742-4658.2010.07800.x
13. Theocharis AD. Versican in health and disease. *Connect Tissue Res*. 2008;49(3):230-234. doi:10.1080/03008200802147571
14. Munkley J, Mills IG, Elliott DJ. The role of glycans in the development and progression of prostate cancer. *Nat Rev Urol*. 2016;13(6):324-333. doi:10.1038/nrurol.2016.65
15. Tuxhorn JA, Ayala GE, Rowley DR. Reactive stroma in prostate cancer progression. *J Urol*. 2001;166(6):2472-2483.
16. Corradi LS, Góes RM, Vilamaior PS, Taboga SR. Increased androgen receptor and remodeling in the prostatic stroma after the inhibition of 5-alpha reductase and aromatase in gerbil ventral prostate. *Microsc Res Tech*. 2009;72:939-950. doi:10.1002/jemt.20740
17. Gallagher J. Fell-Muir lecture: heparan sulphate and the art of cell regulation: a polymer chain conducts the protein orchestra. *Int J Exp Pathol*. 2015;96(4):203-231. doi:10.1111/iep.12135
18. Suhovskih AV, Mostovich LA, Kunin IS, et al. Proteoglycan expression in normal human prostate tissue and prostate cancer. *ISRN Oncol*. 2013;2013:680136. doi:10.1155/2013/680136
19. Ricciardelli C, Quinn DI, Raymond WA, et al. Elevated levels of peritumoral chondroitin sulfate are predictive of poor prognosis in patients treated by radical prostatectomy for early-stage prostate cancer. *Cancer Res*. 1999;59:2324-2328.

20. Sakko AJ, Butler MS, Byers S, et al. Immunohistochemical level of unsulfated chondroitin disaccharides in the cancer stroma is an independent predictor of prostate cancer relapse. *Cancer Epidemiol Biomarkers Prev*. 2008;17(9):2488-2497. doi:10.1158/1055-9965.EPI-08-0204
21. Melrose J. Perlecan, a modular instructive proteoglycan with diverse functional proper. *Int J Biochem Cell Biol*. 2020;128:105849. doi:10.1016/j.biocel.2020.1058
22. Gonçalves BF, Campos SGP, Zanetoni C, et al. A new proposed rodent model of chemically induced prostate carcinogenesis: distinct time-course prostate cancer progression in the dorsolateral and ventral lobes. *Prostate*. 2013;73(11):1202-1213. doi:10.1002/pros.22669
23. Gonçalves BF, Campos SGP, Góes RM, Scarano WR, Taboga SR, Vilamaior PSL. Dual action of high estradiol doses on MNU-induced prostate neoplasms in a rodent model with high serum testosterone: protective effect and emergence of unstable epithelial micro-environment. *Prostate*. 2017;77(9):970-983. doi:10.1002/pros.23353
24. Facina C, Campos SGP, Gonçalves BF, Goes RM, Vilamaior PSL, Taboga SR. Long-term oral exposure to safe dose of bisphenol A in association with high-fat diet stimulate the prostatic lesions in a rodent model for prostate cancer. *Prostate*. 2017;78:152-163. doi:10.1002/pros.23458
25. Campos SGP, Gonçalves BF, Scarano WR, et al. Tissue changes in senescent gerbil prostate after hormone deprivation leads to acquisition of androgen insensitivity. *Int J Exp Pathol*. 2010;91:394-407. doi:10.1111/j.1365-2613.2010.00706.x
26. Campos SG, Gonçalves BF, Scarano WR, Góes RM, Taboga SR. Phenotypic and metabolic aspects of prostatic epithelial cells in aged gerbils after antisteroidal therapy: turnover in the state of chromatin condensation and androgen-independent cell replacement. *Acta Histochem*. 2014;116(1):204-213. doi:10.1016/j.acthis.2013.07.003
27. Scarano WR, Sousa DE, Campos SGP, Corradi LS, Vilamaior PSL, Taboga SR. Oestrogen supplementation following castration promotes stromal remodeling and histopathological alterations in the gerbil ventral prostate. *Int J Exp Pathol*. 2008;89(1):25-37. doi:10.1111/j.1365-2613.2007.00559.x
28. Cordeiro RS, Scarano WR, Campos SG, et al. Androgen receptor in the Mongolian gerbil ventral prostate: evaluation during different phases of postnatal development and following androgen blockage. *Micron*. 2008;39(8):1312-1324. doi:10.1016/j.micron.2008.02.008
29. Pegorin de Campos SG, Zanetoni C, Góes RM, Taboga ST. Biological behavior of the gerbil ventral prostate during postnatal development. *Anat Rec A Discov Mol Cell Evol Biol*. 2006;288:723-733. doi:10.1002/ar.a.20347
30. Pollard M, Suckow MA. Dietary prevention of hormone refractory prostate cancer in Lobund-Wistar rats: a review of studies in a relevant animal model. *Comp Med*. 2006;56:461-467.
31. Weibel ER. Principles and methods for the morphometric study of the lung and other organs. *Lab Invest*. 1963;12:131-155.
32. Scott JE, Dorling J. Differential staining of acid glycosaminoglycans (mucopolysaccharides) by alcian blue in salt solutions. *Histochemie*. 1965;5:221-233. doi:10.1007/BF00306130
33. Scott JE. The molecular biology of histochemical staining by cationic phthalocyanin dyes: the design of replacements for Alcian Blue. *J Microsc*. 1980;119:373-381. doi:10.1111/j.1365-2818.1980.tb04108.x
34. Pinheiro MC, Mora OA, Caldini EG, Battlehner CN, Joazeiro PP, Toledo OMS. Ultrastructural, immunohistochemical and biochemical analysis of glycosaminoglycans and proteoglycans in the mouse pubic symphysis during pregnancy. *Cell Biol Int*. 2005;29(6):458-471. doi:10.1016/j.cellbi.2004.11.025
35. Sakko AJ, Ricciardelli C, Mayne K, et al. Changes in steroid receptors and proteoglycan expression in the guinea pig prostate stroma during puberty and hormone manipulation. *Prostate*. 2007;67(3):288-300. doi:10.1002/pros.20524
36. Della-Colleta HM, Carvalho HF. Hyaluronan content and distribution in the rat ventral prostate after castration. *Biochem Cell Biol*. 2018;96(5):556-563. doi:10.1139/bcb-2017-0242
37. Carvalho HF, Line SR. Basement membrane associated changes in the rat ventral prostate following castration. *Cell Biol Int*. 1996;20(12):809-819. doi:10.1006/cbir.1996.0104
38. Ribeiro DL, Taboga SR, Góes RM. Diabetes induces stromal remodelling and increase in chondroitin sulphate proteoglycans of the rat ventral prostate. *Int J Exp Pathol*. 2009;90(4):400-411. doi:10.1111/j.1365-2613.2009.00657.x
39. Babinski MA, Costa WS, Sampaio FJ, Cardoso LE. Structural organization of fibrous connective tissue in the periacinar region of the transitional zone from normal human prostates as revealed by scanning electron microscopy. *BJU Int*. 2007;100(4):940-944. doi:10.1111/j.1464-410X.2007.07060.x
40. Ricciardelli C, Sakko AJ, Ween MP, Russell DL, Horsfall DJ. The biological role and regulation of versican levels in cancer. *Cancer Metastasis Ver*. 2009;28(1-2):233-245. doi:10.1007/s10555-009-9182-y
41. Ricciardelli C, Mayne K, Sykes PJ, et al. Elevated levels of versican but not decorin predict disease progression in early-stage prostate cancer. *Clin Cancer Res*. 1998;4:963-971.
42. Asimakopoulou AP, Theocharis AD, Tzanakakis GN, Karamanos NK. The biological role of chondroitin sulfate in cancer and chondroitin-based anticancer agentes. *In Vivo*. 2008;22(3):385-389.
43. Gilgunn S, Conroy PJ, Saldova R, Rudd PM, O'Kennedy RJ. Aberrant PSA glycosylation—a sweet predictor of prostate cancer. *Nat Rev Urol*. 2013;10:99-107. doi:10.1038/nrurol.2012.258
44. Schneider M, Khalil AA, Poulton J, et al. Perlecan and Dystroglycan act at the basal side of the Drosophila follicular epithelium to maintain epithelial organization. *Development*. 2006;133:3805-3815. doi:10.1242/dev.02549
45. Yurchenco PD, Patton BL. Developmental and pathogenic mechanisms of basement membrane assembly. *Curr Pharm Des*. 2009;15:1277-1294. doi:10.2174/138161209787846766
46. Lord MS, Tang F, Rnjak-Kovacina J, Smith JGW, Melrose J, Whitelock JM. The multifaceted roles of perlecan in fibrosis. *Matrix Biol*. 2018;68-69:150-166. doi:10.1016/j.matbio.2018.02.013
47. Iozzo RV, Cohen IR, Grässel S, Murdoch AD. The biology of perlecan: the multifaceted heparan sulphate proteoglycan of basement membranes and pericellular matrices. *Biochem J*. 1994;302(pt 3):625-639. doi:10.1042/bj3020625
48. Savoré C, Zhang C, Muir C, et al. Perlecan knockdown in metastatic prostate cancer cells reduces heparin-binding growth factor responses in vitro and tumor growth in vivo. *Clin Exp Metastasis*. 2005;22:377-390. doi:10.1007/s10585-005-2339-3
49. Petraki CD, Sfikas CP. Histopathological changes induced by therapies in the benign prostate and prostateadenocarcinoma. *Histol Histopathol*. 2007;22(1):107-118. doi:10.14670/HH-22.107
50. Esser AK, Cohen MB, Henry MD. Dystroglycan is not required for maintenance of the luminal epithelial basement membrane or cell polarity in the mouse prostate. *Prostate*. 2010;70(7):777-787. doi:10.1002/pros.21110
51. Datta MW, Hernandez AM, Schlicht MJ, et al. Perlecan, a candidate gene for the CAPB locus, regulates prostate cancer cell growth via the Sonic Hedgehog pathway. *Mol Cancer*. 2006;5:9. doi:10.1186/1476-4598-5-9
52. Goes RM, Zanetoni C, Tomiosso TC, Ribeiro DL, Taboga SR. Surgical and chemical castration induce differential histological response in

prostate lobes of Mongolian gerbil. *Micron*. 2007;38(3):231-236. doi:10.1016/j.micron.2006.06.016

53. Arcadi JA. Extracellular matrix in prostate adenocarcinoma: changes in the glycoprotein component of the basement membrane. *Urol Oncol*. 1997;3:113-117. doi:10.1016/s1078-1439(98)00010-6
54. Edwards IJ. Proteoglycans in prostate cancer. *Nat Rev Urol*. 2012;9(4):196-206. doi:10.1038/nrurol.2012.19

How to cite this article: Campos SGP, Gonçalves BF, Ruiz TFR, et al. Proteoglycans orchestrate remodeling of prostatic cytoarchitecture after androgenic blockade in old gerbils. *The Prostate*. 2023;83:179-189. doi:10.1002/pros.24451